

Supporting Information

Optimized Hierarchical Nickel Sulfide as Highly Active Bifunctional Catalyst for Overall Water Splitting

Yun Tong,^{a,b} and Pengzuo Chen,^{b}*

^a Department of Chemistry, Key Laboratory of Surface & Interface Science of Polymer Materials of Zhejiang Province, Zhejiang Sci-Tech University, Hangzhou 310018, China

^b Institute of Chemical Sciences and Engineering, École Polytechnique Fédérale de Lausanne (EPFL), 1015 Lausanne, Switzerland.

Correspondence and requests for materials should be addressed to P. Z. Chen (E-mail: pzchen@mail.ustc.edu.cn)

Table of contents

Figure S1 The XRD pattern of c-Ni ₃ S ₂ /NF electrode.	3
Figure S2 The EIS spectrum of for all prepared electrodes at the potential of -0.2 V.	3
Figure S3 The OER polarization curves of a-Ni ₃ S ₂ /NF, b-Ni ₃ S ₂ /NF, c-Ni ₃ S ₂ /NF and d-Ni ₃ S ₂ /NF electrodes in 1 M KOH solution.	4
Figure S4 a) The TEM image and high resolution XPS spectra of b) Ni 2p, c) Fe 2p and d) S 2p of FeOOH coated c-Ni ₃ S ₂ sample.....	5
Figure S5 The corresponding Tafel slopes of all prepared Fe-Ni ₃ S ₂ /NF electrodes for OER.	6
Figure S6 The EIS spectra of all prepared Fe-Ni ₃ S ₂ /NF electrodes at potential of 1.47 V for OER.	6
Figure S7 Cyclic voltammograms of a) Fe-a-Ni ₃ S ₂ /NF, b) Fe-b-Ni ₃ S ₂ /NF, c) Fe-c-Ni ₃ S ₂ /NF and d) Fe-d-Ni ₃ S ₂ /NF electrodes at different scan rates from 20 to 100 mV s ⁻¹	7
Figure S8 The ECSA values of all prepared Fe-Ni ₃ S ₂ /NF electrodes.....	8
Figure S9 The ECSA normalized OER performance of all prepared Fe-Ni ₃ S ₂ /NF electrodes.....	8
Figure S10 TEM image and elemental mapping images of Fe-a-Ni ₃ S ₂ catalyst after OER test.	9
Figure S11 TEM image and elemental mapping images of Fe-b-Ni ₃ S ₂ catalyst after OER test.	10
Figure S12 TEM image and elemental mapping images of Fe-d-Ni ₃ S ₂ catalyst after OER test.	11
Figure S13 The XPS survey of Fe-c-Ni ₃ S ₂ /NF catalyst after OER test.	12
Figure S14 The high resolution XPS spectrum of O 1s for Fe-c-Ni ₃ S ₂ /NF catalyst after OER test.	12
Figure S15 The Raman spectrum of Fe-c-Ni ₃ S ₂ /NF catalyst after OER test.	13
Table S1. The comparison of the OER performance of Fe-Ni based catalysts with other state-of-the-art electrocatalysts.	14
Table S2. The element contents of all prepared Fe-Ni ₃ S ₂ catalysts after OER activation.	15
References	16

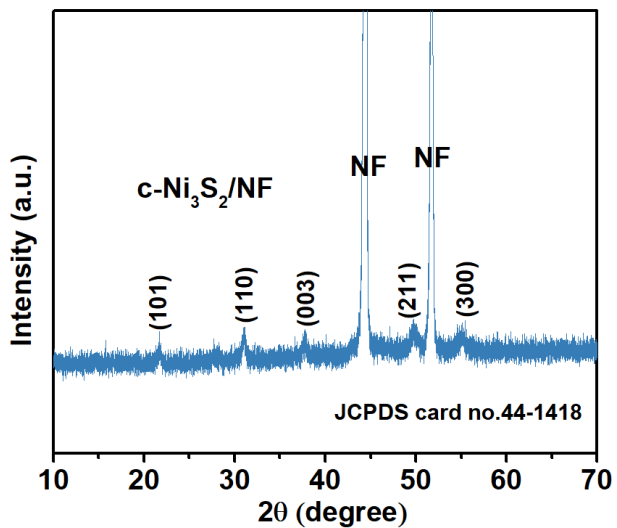


Figure S1 The XRD pattern of $c\text{-Ni}_3\text{S}_2/\text{NF}$ electrode.

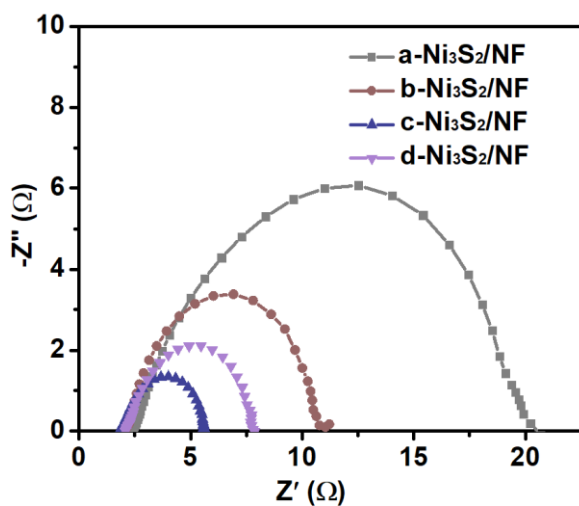


Figure S2 The EIS spectrum of for all prepared electrodes at the potential of -0.2 V.

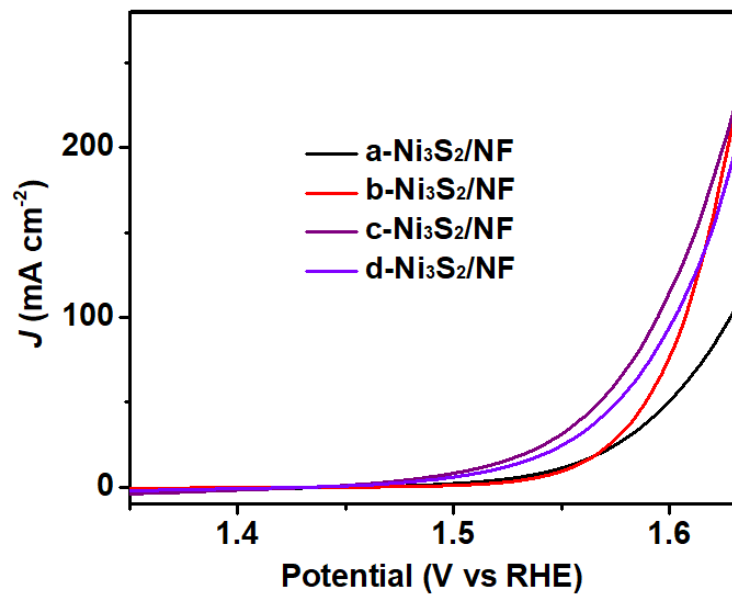


Figure S3 The OER polarization curves of a- $\text{Ni}_3\text{S}_2/\text{NF}$, b- $\text{Ni}_3\text{S}_2/\text{NF}$, c- $\text{Ni}_3\text{S}_2/\text{NF}$ and d- $\text{Ni}_3\text{S}_2/\text{NF}$ electrodes in 1 M KOH solution.

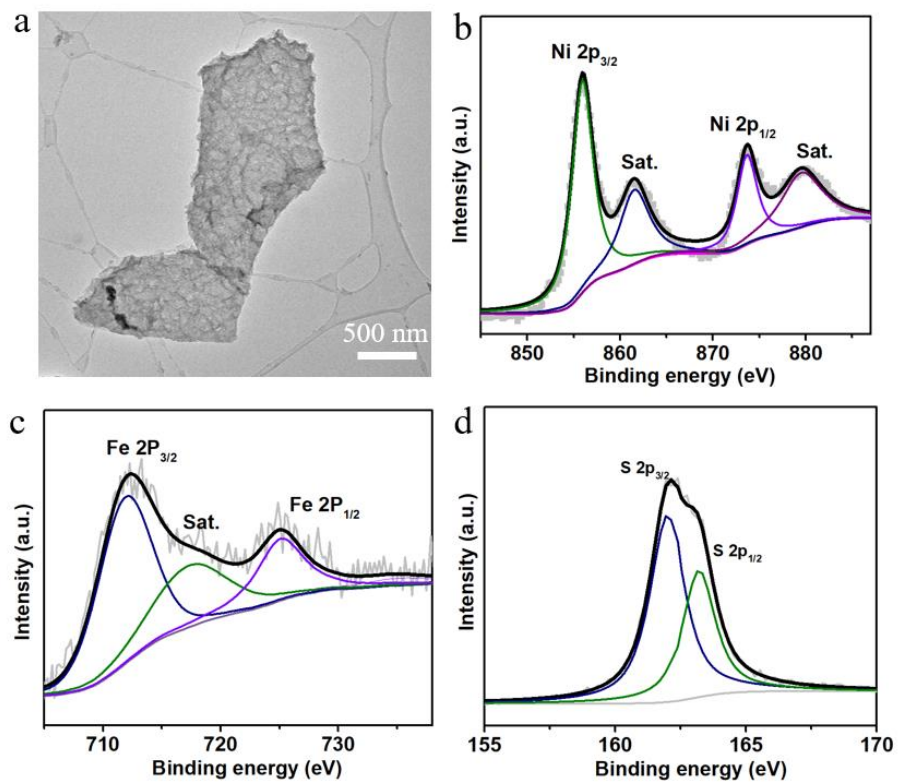


Figure S4 a) The TEM image and high resolution XPS spectra of b) Ni 2p, c) Fe 2p and d) S 2p of FeOOH coated c-Ni₃S₂ sample.

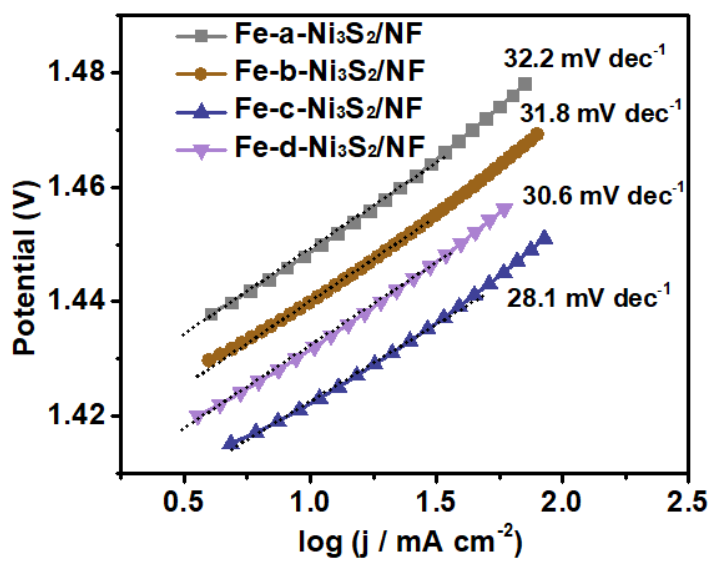


Figure S5 The corresponding Tafel slopes of all prepared Fe-Ni₃S₂/NF electrodes for OER.

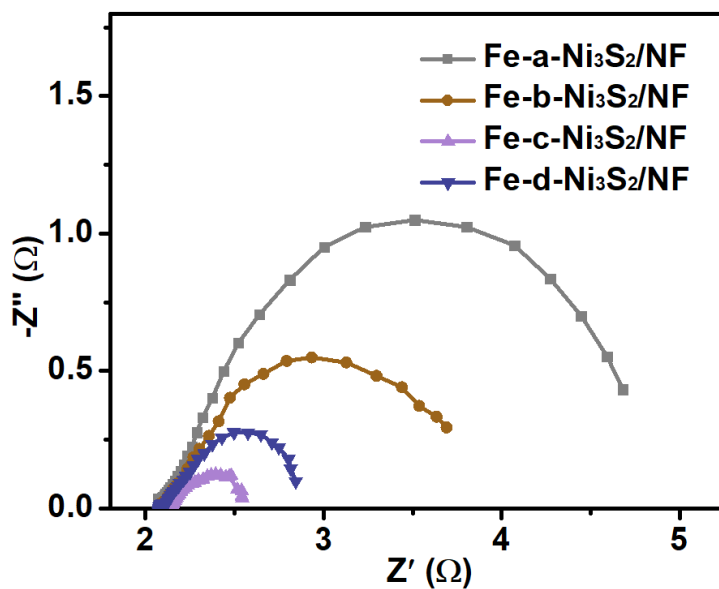


Figure S6 The EIS spectra of all prepared Fe-Ni₃S₂/NF electrodes at potential of 1.47 V for OER.

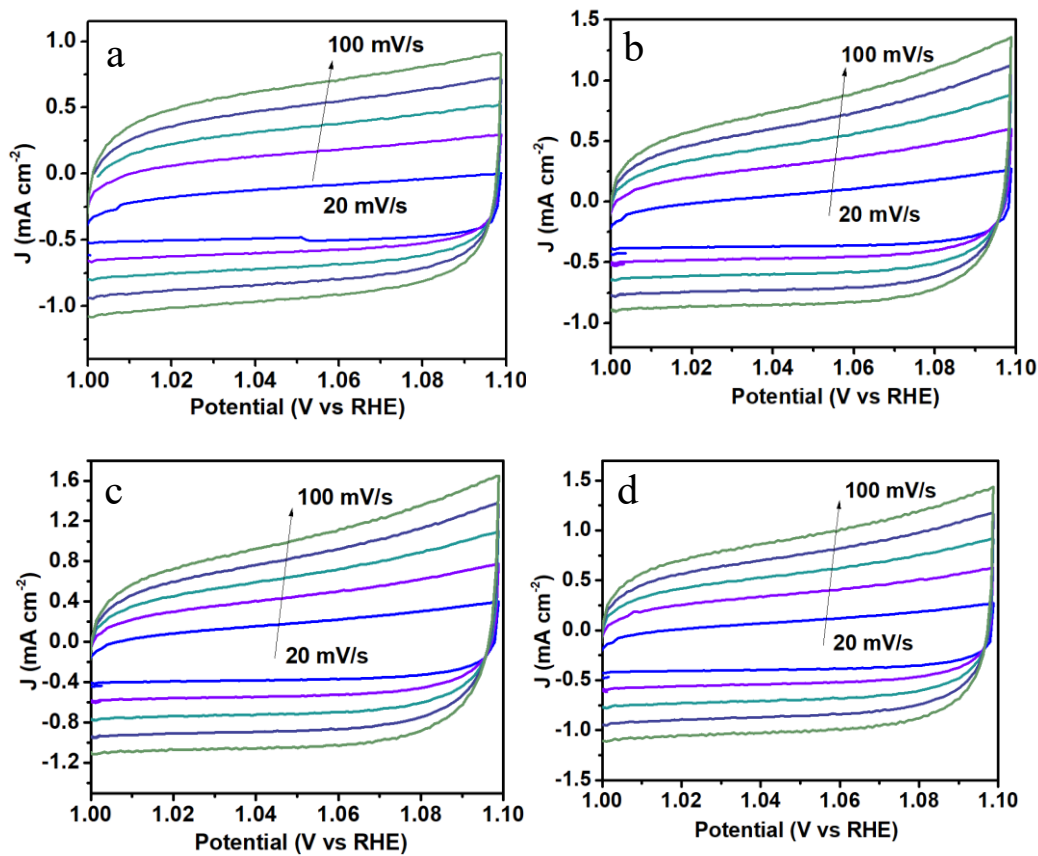


Figure S7 Cyclic voltammograms of a) Fe-a- $\text{Ni}_3\text{S}_2/\text{NF}$, b) Fe-b- $\text{Ni}_3\text{S}_2/\text{NF}$, c) Fe-c- $\text{Ni}_3\text{S}_2/\text{NF}$ and d) Fe-d- $\text{Ni}_3\text{S}_2/\text{NF}$ electrodes at different scan rates from 20 to 100 mV s^{-1} .

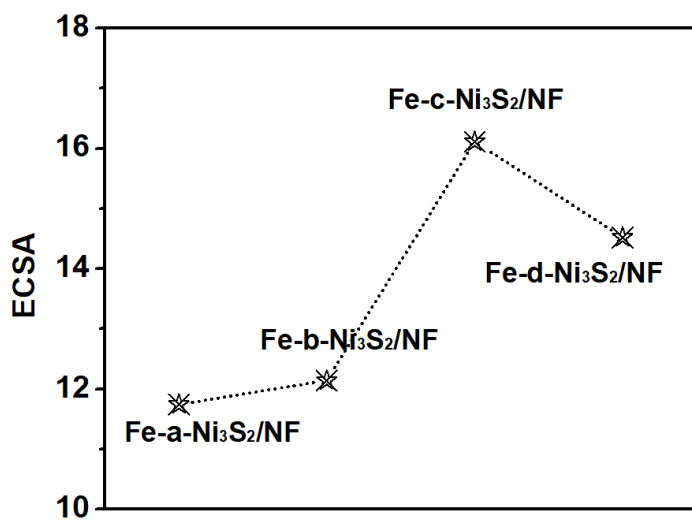


Figure S8 The ECSA values of all prepared Fe-Ni₃S₂/NF electrodes.

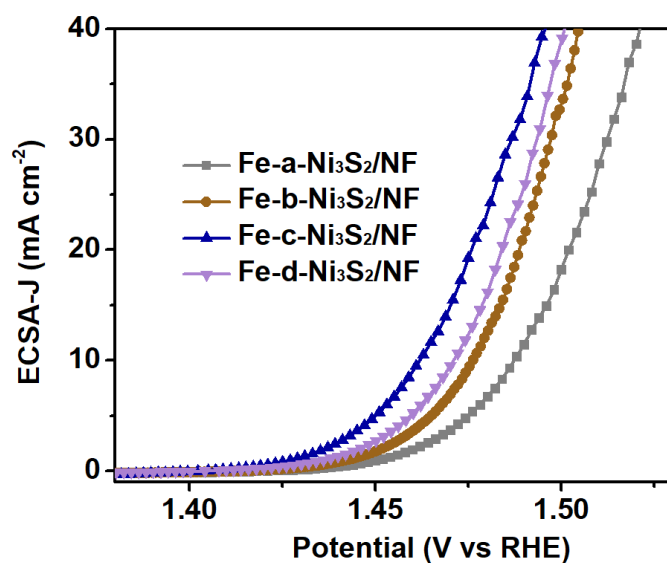


Figure S9 The ECSA normalized OER performance of all prepared Fe-Ni₃S₂/NF electrodes.

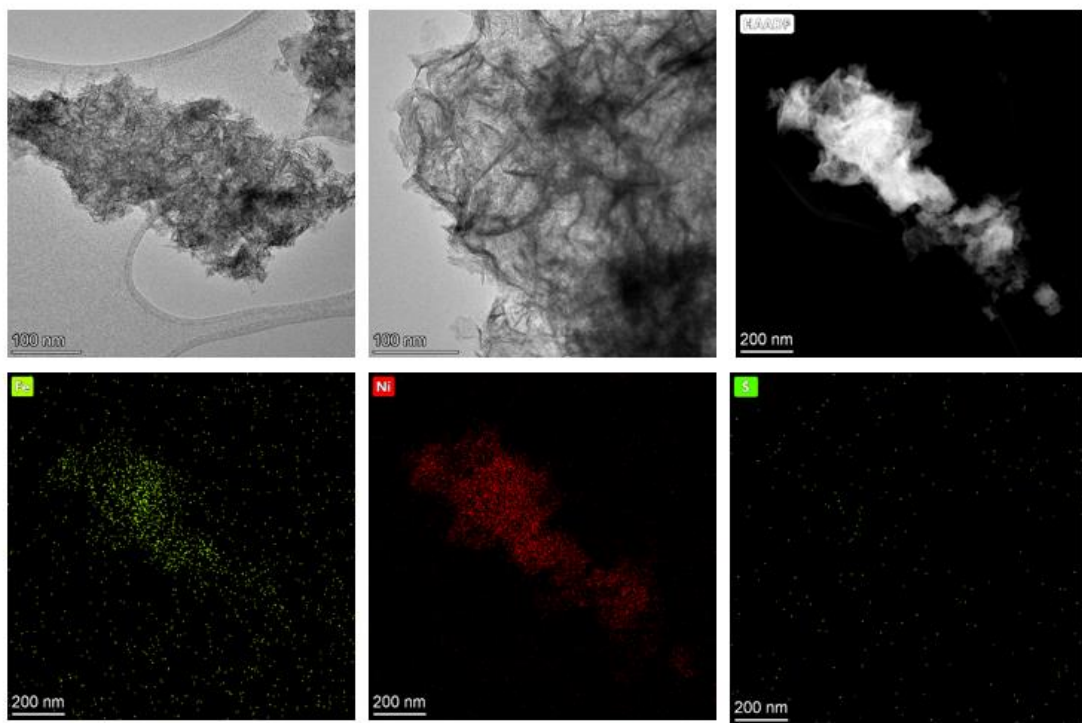


Figure S10 TEM image and elemental mapping images of Fe-a-Ni₃S₂ catalyst after OER test.

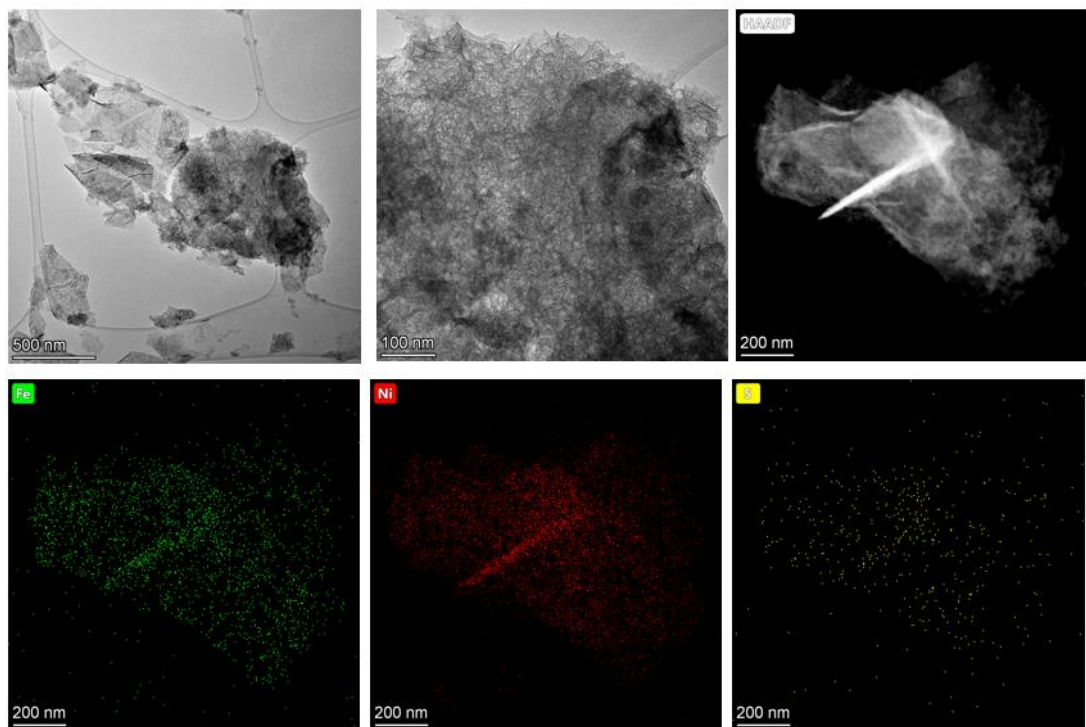


Figure S11 TEM image and elemental mapping images of Fe-b-Ni₃S₂ catalyst after OER test.

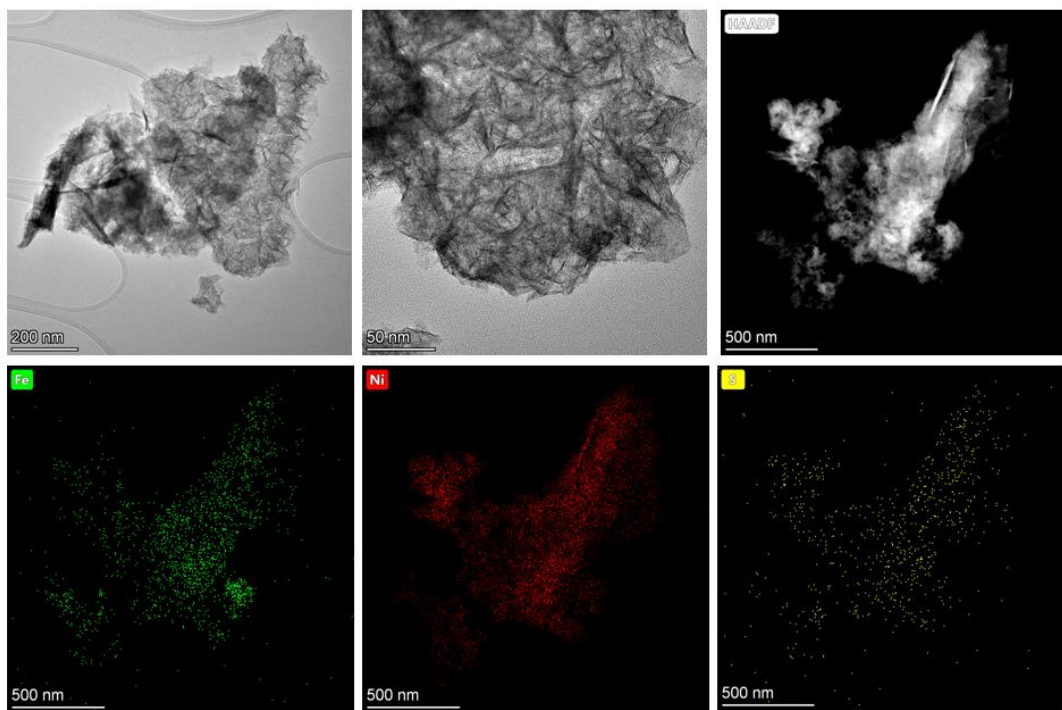


Figure S12 TEM image and elemental mapping images of Fe-d-Ni₃S₂ catalyst after OER test.

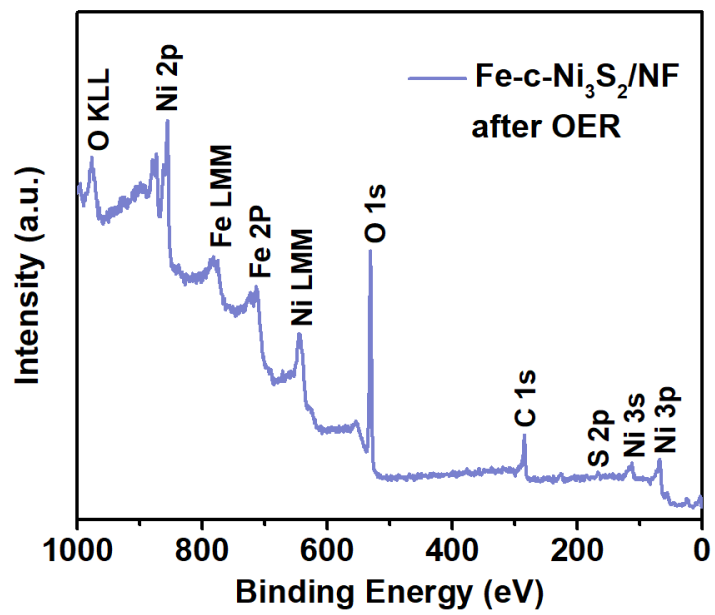


Figure S13 The XPS survey of Fe-c-Ni₃S₂/NF catalyst after OER test.

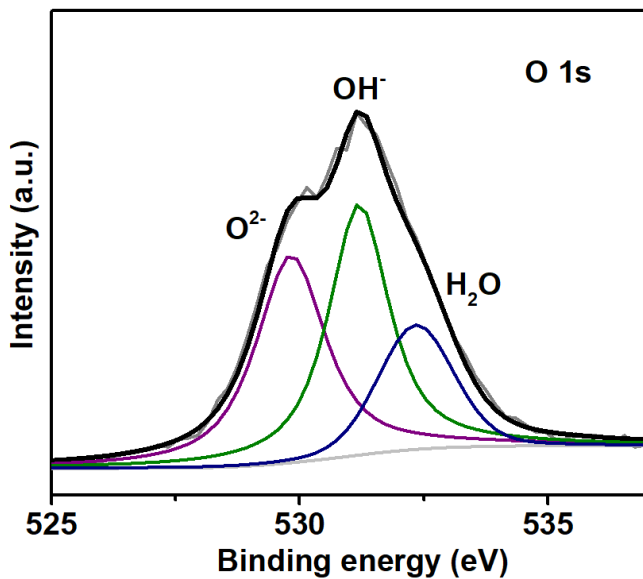


Figure S14 The high resolution XPS spectrum of O 1s for Fe-c-Ni₃S₂/NF catalyst after OER test.

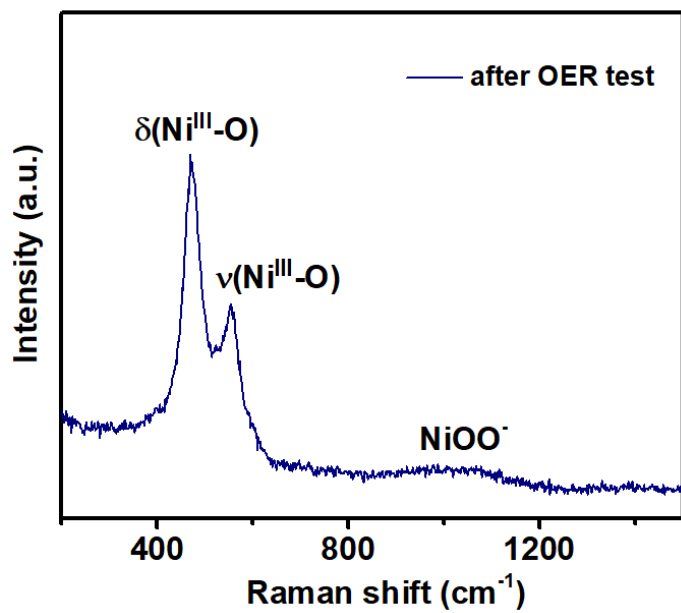


Figure S15 The Raman spectrum of Fe-c-Ni₃S₂/NF catalyst after OER test.

Table S1. The comparison of the OER performance of Fe-Ni based catalysts with other state-of-the-art electrocatalysts.

Catalysts	η_{10} (mV)	η_{100} (mV)	Tafel slope (mV dec ⁻¹)	Electrodes	References
Fe-c-Ni ₃ S ₂	193	222	28.1	NF	This work
Fe-doped β -Ni(OH) ₂	219	280	53.0	NF	[1]
NiFeO _x	230	271	31.5	CFP	[2]
NiFe hydroxides	245	280	28.0	NF	[3]
Ni-Fe LDH hollow prisms	280	370	49.4	GC	[4]
DR-Ni ₃ FeN/N-G	250	310	38.0	RDE	[5]
Fe ²⁺ -NiFe LDH	195	/	40.3	CFP	[6]
NiFe _{0.8} Ce _{0.2}	197	280	59.0	NF	[7]
NiZnFeB-LDH	/	280	48.4	NF	[8]
fcc-NiFe@NC	226	263	41	CC	[9]
Ni _{0.8} Fe _{0.2} -AHNA	190	248	34.7	NF	[10]
AN-CuNiFe	224	/	44	GC	[11]
Ni-Fe-2	219	280	53.0	NF	[12]
NF-AC-NiO _x -Fe	215	248	34.0	NF	[13]
Ni ₆₀ Fe ₃₀ Mn ₁₀	208	270	62.0	Alloy Foam	[14]
NiFe LDH@Ni ₃ N	/	238	61.0	NF	[15]
NiFeRu-LDH	225	260	/	NF	[16]

Table S2. The element contents of all prepared Fe-Ni₃S₂ catalysts after OER activation.

Catalysts/Elements	EDS (%)			
	Ni	Fe	S	O
Fe-a-Ni ₃ S ₂	37.8	12.2	0.2	49.8
Fe-b-Ni ₃ S ₂	38.0	11.8	1.1	49.1
Fe-c-Ni ₃ S ₂	37.5	12.0	2.8	47.7
Fe-d-Ni ₃ S ₂	37.2	11.9	3.0	47.9

References

- [1] T. Kou, S. Wang, J.L. Hauser, M. Chen, S.R.J. Oliver, Y. Ye, J. Guo, Y. Li, Ni Foam-Supported Fe-Doped β -Ni(OH)₂ Nanosheets Show Ultralow Overpotential for Oxygen Evolution Reaction, *ACS Energy Lett.* 4 (2019) 622–628.
- [2] H. Wang, H.-W. Lee, Y. Deng, Z. Lu, P.-C. Hsu, Y. Liu, D. Lin, Y. Cui, Bifunctional non-noble metal oxide nanoparticle electrocatalysts through lithium-induced conversion for overall water splitting, *Nat. Commun.* 6 (2015) 7261.
- [3] R.A. Senthil, J. Pan, X. Yang, Y. Sun, Nickel foam-supported NiFe layered double hydroxides nanoflakes array as a greatly enhanced electrocatalyst for oxygen evolution reaction, *Int. J. Hydrogen Energy.* 43 (2018) 21824–21834.
- [4] L. Yu, J.F. Yang, B.Y. Guan, Y. Lu, X.W.D. Lou, Hierarchical Hollow Nanoprism Based on Ultrathin Ni-Fe Layered Double Hydroxide Nanosheets with Enhanced Electrocatalytic Activity towards Oxygen Evolution, *Angew. Chemie - Int. Ed.* 57 (2018) 172–176.
- [5] S. Zhao, M. Li, M. Han, D. Xu, J. Yang, Y. Lin, N.-E. Shi, Y. Lu, R. Yang, B. Liu, Z. Dai, J. Bao, Defect-Rich Ni₃FeN Nanocrystals Anchored on N-Doped Graphene for Enhanced Electrocatalytic Oxygen Evolution, *Adv. Funct. Mater.* 28 (2018) 1706018.
- [6] M. Wang, Introducing Fe²⁺ into Nickel-Iron Layered Double Hydroxide : Local Structure Modulated Water Oxidation Activity, *Angew. Chem. Int. Ed.* 57 (2018) 9392.
- [7] H.S. Jadhav, A. Roy, B.Z. Desalegan, J.G. Seo, An advanced and highly efficient Ce assisted NiFe-LDH electrocatalyst for overall water splitting, *Sustain. Energy Fuels.* 4 (2020) 312–323.
- [8] J. He, P. Xu, J. Sun, Fe and B Codoped Nickel Zinc Layered Double Hydroxide for Boosting the Oxygen Evolution Reaction, *ACS Sustain. Chem. Eng.* 8 (2020) 2931–2938.
- [9] C. Wang, H. Yang, Y. Zhang, Q. Wang, NiFe Alloy Nanoparticles with hcp

Crystal Structure Stimulate Superior Oxygen Evolution Reaction Electrocatalytic Activity, *Angew. Chemie Int. Ed.* 58 (2019) 6099–6103.

- [10] C. Liang, P. Zou, A. Nairan, Y. Zhang, J. Liu, K. Liu, S. Hu, F. Kang, H.J. Fan, C. Yang, Exceptional performance of hierarchical Ni–Fe oxyhydroxide@NiFe alloy nanowire array electrocatalysts for large current density water splitting, *Energy Environ. Sci.* 13 (2020) 86–95.
- [11] C.G. Morales-Guio, L. Liardet, X. Hu, Oxidatively Electrodeposited Thin-Film Transition Metal (Oxy)hydroxides as Oxygen Evolution Catalysts, *J. Am. Chem. Soc.* 138 (2016) 8946–8957.
- [12] Y. Hou, M.R. Lohe, J. Zhang, S. Liu, X. Zhuang, X. Feng, Vertically oriented cobalt selenide/NiFe layered-double-hydroxide nanosheets supported on exfoliated graphene foil: an efficient 3D electrode for overall water splitting, *Energy Environ. Sci.* 9 (2016) 478–483.
- [13] F. Song, M.M. Busch, B. Lassalle-Kaiser, C.-S. Hsu, E. Petkucheva, M. Bensimon, H.M. Chen, C. Corminboeuf, X. Hu, An Unconventional Iron Nickel Catalyst for the Oxygen Evolution Reaction, *ACS Cent. Sci.* 5 (2019) 558–568.
- [14] E. Detsi, J.B. Cook, B.K. Lesel, C.L. Turner, Y.-L. Liang, S. Robbennolt, S.H. Tolbert, Mesoporous Ni₆₀Fe₃₀Mn₁₀-alloy based metal/metal oxide composite thick films as highly active and robust oxygen evolution catalysts, *Energy Environ. Sci.* 9 (2016) 540–549.
- [15] B. Wang, S. Jiao, Z. Wang, M. Lu, D. Chen, Y. Kang, G. Pang, S. Feng, Rational design of NiFe LDH@Ni₃N nano/microsheet arrays as a bifunctional electrocatalyst for overall water splitting, *J. Mater. Chem. A.* 8 (2020) 17202–17211.
- [16] G. Chen, T. Wang, J. Zhang, P. Liu, H. Sun, X. Zhuang, M. Chen, X. Feng, Accelerated Hydrogen Evolution Kinetics on NiFe-Layered Double Hydroxide Electrocatalysts by Tailoring Water Dissociation Active Sites, *Adv. Mater.* 30 (2018) 1706279.